Diode-pumped Pr^{3+}:$LiYF_4$ continuous-wave deep red laser at 698 nm

Zhe Liu,[1] Zhiping Cai,[1,*] Shunlin Huang,[1] Chenghang Zeng,[1] Zengyou Meng,[1] Yikun Bu,[1] Zhengqian Luo,[1] Bin Xu,[1] Huiying Xu,[1] Chenchun Ye,[1] Florent Stareki,[2] Patrice Camy,[2] and Richard Moncorgé[2]

[1]*Department of Electronic Engineering, Xiamen University, Xiamen, Fujian 361005, China*
[2]*Centre de Recherche sur les Ions, les Matériaux et la Photonique (CIMAP) UMR CEA-CNRS-ENSICaen, Université de Caen, Caen 14050, France*
**Corresponding author: zpcai@xmu.edu.cn*

Received November 16, 2012; revised December 5, 2012; accepted December 7, 2012; posted December 10, 2012 (Doc. ID 180085); published January 9, 2013

We report continuous-wave laser operation at 698 nm in Pr^{3+}-doped $LiYF_4$ crystal using an InGaN laser diode emitting at 444 nm with a maximum output power of 760 mW. By suppressing the oscillation at 640 and 721 nm, a maximum output power of 156 mW at 698 nm was obtained in a single transverse mode with a slope efficiency as high as 48.7%. The beam quality factors M^2 in the x and y directions were measured to be 1.4 and 1.2, respectively.

OCIS codes: 140.3480, 140.3580, 140.7300.

1. INTRODUCTION

In recent years, great interest has been paid to Pr^{3+}-doped materials, because they can offer a large range of laser transitions in the blue, green, orange, red, and deep red spectral regions. In order to achieve these visible lasers, the Pr^{3+} ions need to be pumped from their $^3H_4$ ground level to their $^3P_0$ (around 480 nm), $^3P_1 + {}^1I_6$ (around 469 nm), or $^3P_2$ (around 444 nm) excited energy level. Correspondingly, three effective pump sources have been developed to satisfy the pumping requirements, i.e., optically pumped and frequency-doubled semiconductor lasers at ~480 nm [1], a diode-pumped and frequency-doubled Nd:YAG at ~469 nm [2,3], and InGaN laser diodes at ~444 nm [4–13]. Among them, the most commonly used ones are the InGaN-based laser diodes, mainly because of their compactness and commercial availability. Pumping with such InGaN laser diodes, laser actions in several Pr^{3+}-doped materials, such as $LiYF_4$ (YLF) [4–6], $LiLuF_4$ [6], $LiGdF_4$ [6], BaY_2F_8 [7], KY_3F_{10} [8], $YAlO_3$ [9], $SrAl_{12}O_{19}$[10], and fluoride fibers [11,12], have been reported. Compared with the oxide hosts, the fluoride hosts, particularly YLF, have been found to be the most promising host materials for Pr^{3+}-based solid-state lasers, since Pr^{3+}-doped fluorides have lower nonradiative multiphonon decay and lower excited state absorption from the upper laser levels. Recently, really efficient diode-pumped continuous-wave (cw) laser oscillations of Pr:YLF on several transitions have been demonstrated [13].

However, in all these previous works, the deep red laser emission on the $^3P_0 \rightarrow {}^3F_3$ transition of Pr^{3+} is rarely considered. In Pr^{3+}-doped fluoride crystals, this transition emits at around 698 nm, which may be of particular interest in some specific applications. For example, a frequency-stabilized laser at 698 nm is a key component for the construction of the optical frequency standards based on strontium atoms [14]. The frequency-doubled laser at 349 nm is also expected to generate many applications for analytical chemistry, genomics, and matrix-assisted laser desorption/ionization. This 349 nm laser emission was already obtained by frequency-tripling a Nd:YLF laser, but it was relatively inefficient and complicated. Pr^{3+}-based cw solid-state lasers emitting on the $^3P_0 \rightarrow {}^3F_3$ transition were only presented in two previous works [15,16], and both of them operated by pumping Pr:YLF laser crystals with an Ar^+ ion laser, which is both cumbersome and inefficient, due to the poor overlap between the pump laser and Pr^{3+} absorption spectral ranges. Consequently, only a maximum output power of 71 mW and a slope efficiency of 10.3% [15] could be obtained.

In this paper, we present the realization of a compact and efficient InGaN laser-diode-pumped Pr:YLF deep red laser at about 698 nm. To the best of our knowledge, it is the first demonstration of a diode-pumped Pr^{3+} laser on the considered $^3P_0 \rightarrow {}^3F_3$ transition. A maximum output power of 156 mW is obtained with a slope efficiency as high as 48.7%.

2. EXPERIMENTAL CONDITIONS

A. Active Medium and Pumping Source

The laser gain medium is a 5 mm × 4 mm × 4 mm (5 mm in thickness), 0.5 at. % Pr^{3+}-doped YLF crystal, which was grown by the Czochralski method in a Chinese lab. No particular effort has been made to optimize the Pr^{3+} doping concentration and crystal length. The laser crystal, having uncoated, parallel, and well-polished end facets, was cut perpendicularly to the crystallographic a axis. This allowed us to pump and lase the crystal in the π (E parallel to c) as well as in the σ (E perpendicular to c) polarization. The polarized absorption spectra were registered by using a PerkinElmer UV–visible–NIR Lambda-750 spectrophotometer. The partial spectra in the blue region are reported in Fig. 1. The π-polarized absorption spectrum peaks at 444 nm with an absorption coefficient of 3.6 cm^{-1}, whereas the σ-polarized one at the same wavelength of 444 nm has an absorption coefficient of 1.0 cm^{-1}. On the other hand, the absorbed pump power in

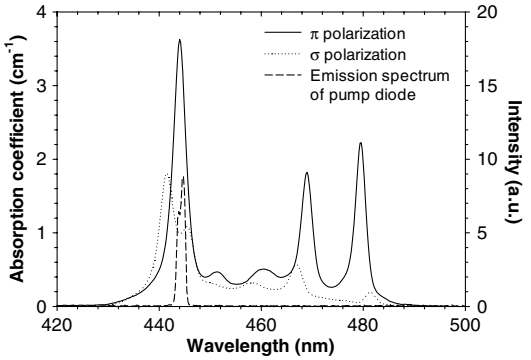

Fig. 1. Absorption spectrum of the 5 mm long Pr:YLF crystal (0.5 at. %) at room temperature, along with the emission spectrum of the pump diode.

π polarization, which can be estimated by measuring the values of the incident pump power (P_{in}) and transmitted pump power (P_{trans}) after a single pass through the Pr:YLF crystal, and by using the expression $(1-R)^2 \exp(-\alpha l) = P_{\text{trans}}/P_{\text{in}}$ (where R is the Fresnel reflection coefficient), led to an effective absorption coefficient of about 2.5 cm^{-1}. This value was found to be lower than the actual peak absorption coefficient, probably because of the linewidth of the laser diode (1.7 nm, as shown in Fig. 1).

A commercially available InGaN laser diode was employed as the pumping source. The beam quality of the InGaN laser diode expressed by the beam propagation factor M^2 was determined to be 2.1 and 4.3 in the x and y directions, respectively. The pump beam is shaped close to an ellipse, and no ripple-like beam has been observed either in the horizontal or in the vertical direction. This beam property is different from that indicated in other publications (see, e.g., [7]). It means a relatively good pump beam quality, which is helpful in the overlap between the pump beam and laser modes. During the experiments, we have not utilized any pump beam reshaper, only a collimating lens (L1) and a focusing lens (L2) (see in Fig. 2).

The wavelength of the laser diode does not change significantly with the temperature [4]; it mainly depends on the driving current. It was found, however, that the pump wavelength shifted to ~444 nm, which corresponds to a maximum of the $^3H_4$ to $^3P_2$ absorption transition of Pr:YLF, when the driving current was set at its highest value. Hence, to maximize the absorbed pump power in order to produce the optimal laser performance, we fixed the driving current of the InGaN laser diode at its highest value during the laser experiments, and the input pump power was simply varied by using a variable metallic neutral density filter placed before the focusing lens (L2). In this way, the result showed that ~66% of the pump power was absorbed in the laser crystal.

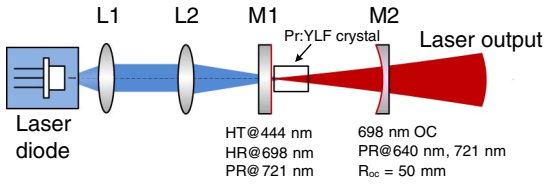

Fig. 2. (Color online) Schematic layout of the diode-pumped Pr:YLF laser at 698 nm. L1, collimating lens; L2, focusing lens; M1, input mirror; M2, output coupler; HT, high transmission; HR, high reflection; PR, partial reflection.

B. Cavity Configuration

Figure 2 shows a schematic of the laser setup. A simple and compact plano-concave resonator with an output mirror of 50 mm in radius of curvature was used. After collimation with lens L1, the pump beam was focused into the laser crystal by using an antireflection-coated spherical lens L2 with a focal length of 50 mm. The crystal was mounted on a copper heat sink without any additional cooling. The crystal was oriented such that the pump beam was polarized in the direction parallel to the crystallographic c axis (π polarization) for maximum absorption at 444 nm.

According to the previous literature [13], the stimulated emission cross section for the $^3P_0 \rightarrow {}^3F_3$ transition line at 698 nm, which is more particularly considered in the present article, should be around 5×10^{-20} cm^2 in the π polarization. Our measurements (emission spectra registered with better defined polarizations and calibrated by using carefully estimated branching ratios, which will be published in a subsequent article) indicate some different emission cross sections of Pr:YLF compared to [13]. Although these measurements show a different emission cross section of $^3P_0 \rightarrow {}^3F_3$, which is about 6.5×10^{-20} cm^2, this cross section remains substantially smaller than the stimulated emission cross sections of the other transitions $^3P_0 \rightarrow {}^3F_2$ and $^3P_0 \rightarrow {}^3F_4$, peaking at 639.6 and 720.8 nm, respectively. This means that it is crucial to avoid lasing from these other laser transitions with larger emission cross sections. For that purpose, we used specifically coated mirrors rather than any intracavity wavelength selective elements, as reported in [16]. The input mirror (M1) had a high transmission of $T > 97\%$ at 444 nm, a high reflection of $R > 99.9\%$ around 698 and 640 nm, and $T > 4\%$ around 721 nm. The 721 nm laser emission was suppressed mainly by the input mirror (M1), and the output mirrors (M2) also had partial transmissions at 721 nm. The 640 nm laser emission was really suppressed, thanks to the transmission of the output mirrors (M2). Two output mirrors were utilized with transmissions of 0.5% and 0.9% at 698 nm. The output mirror with a transmission of 0.5% at 698 nm has transmissions of about 42% and 0.5% at 640 and 721 nm, respectively. The output mirror with a transmission of 0.9% has transmissions of about 4.5% and 1.5% at 640 and 721 nm, respectively.

The measured pump beam focus sizes inside the laser crystal were about 67 and 61 μm in the x and y orientations, respectively. The resonator length was around 45 mm when maximum output power was obtained. In such conditions, the laser beam size in the crystal was estimated (by using the standard ABCD matrix technique) to be about 63 μm, attesting to a good pump-and-laser mode overlap in the beam profiles and allowing for an optimal energy extraction from the gain medium.

3. LASER RESULTS

The output spectrum was measured with an Advantest Q8384 optical spectrum analyzer. It was recorded at the maximum output power for the mirror with $T = 0.9\%$, and the spectra look identical for both output couplers. The result is shown in Fig. 3. Laser oscillation occurred in the $^3P_0 \rightarrow {}^3F_3$ transition of Pr^{3+} at 698 nm in π polarization. No lasing at 640 or 721 nm was observed. The main diagram of Fig. 3 gives the details of the laser spectrum at 698 nm with a spectral resolution of 10 pm. The central laser emission wavelength was measured

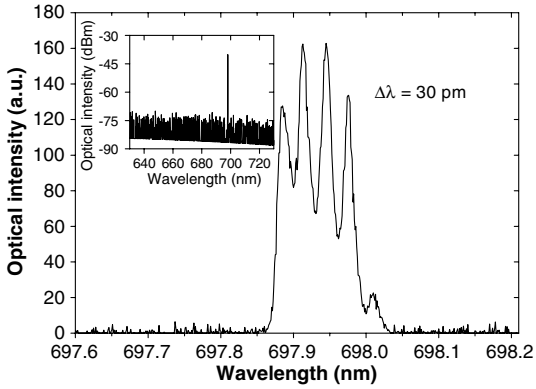

Fig. 3. Output spectrum of the Pr:YLF laser at 698 nm with a resolution of 0.01 nm. Inset shows the output spectrum with a resolution of 0.14 nm.

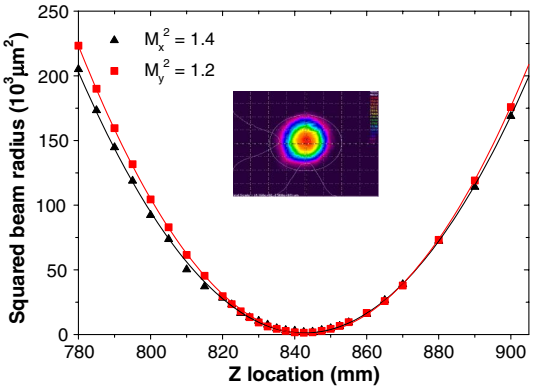

Fig. 5. (Color online) Squared beam radius of the output laser as a function of the z axis location.

to be 697.95 nm with a spectral width (FWHM) of 0.10 nm. The laser spectrum is composed of five peaks, and the wavelength separation of two adjacent peaks is ~30 pm. This wavelength interval corresponds to an etalon effect in the Pr:YLF crystal, whose free spectral range (FSR) can be obtained by calculating $\Delta\nu = c/2nL_c$, where c is the speed of light, $n = 1.47$ is the refractive index of Pr:YLF at 698 nm in π polarization, and $L_c = 5$ mm is the length of the crystal. The FSR of the etalon is calculated to be 20.39 GHz, corresponding to a wavelength interval of 33 pm, which is close to the measured wavelength interval of 30 pm.

Figure 4 shows the 698 nm laser output power as a function of absorbed pump power for the two output coupler transmissions. These curves indicate that the most efficient laser operation is achieved by using a 0.9% coupling. The maximum output power of 156 mW was obtained under an absorbed pump power of 497 mW with a slope efficiency of 48.7% with respect to the absorbed pump power, and the absorbed threshold pump power was 138 mW. By using the 0.5% output coupling, the maximum output power was 115 mW, with a slope efficiency and an absorbed threshold pump power of 26.9% and 47 mW, respectively. Substituting the measured slope efficiency values into the theoretical expression for the laser slope efficiency,

$$\eta_{\text{slope}} = \varepsilon_P \eta_S [T/(T+L)],$$

where ε_P is the pump efficiency of the $^3P_0$ emitting level after pumping into the $^3P_2$, a pump efficiency that is assumed to be equal to 1, and $\eta_S = \lambda_P/\lambda_L = 63.6\%$ is the Stokes factor. We have estimated, using the data obtained with the 0.9% output coupling, round-trip internal losses of about 0.3%. If the data with the 0.5% output coupling are used, the round-trip internal losses are estimated to be about 0.7%. These results are comparable with those of the previous work on the $^3P_0 \rightarrow {}^3F_2$ transition using a crystal of the same length [3] but are bigger than those of the work using a 2.9 mm long crystal [13].

Finally, the laser beam has been characterized spatially. A laser beam analyzer (Spiricon M^2 – 200, using the 90/10 knife-edge method) was employed to measure the beam quality. Figure 5 shows the squared beam radius for the laser beam. The values of M^2 in the x and y directions were measured to be 1.4 and 1.2, respectively. Moreover, the transverse spatial profile of the laser beam was measured with a CCD camera (MicronViewer 7290A). The result is shown in the inset in Fig. 5, indicating a near-diffraction-limited TEM_{00} transverse mode.

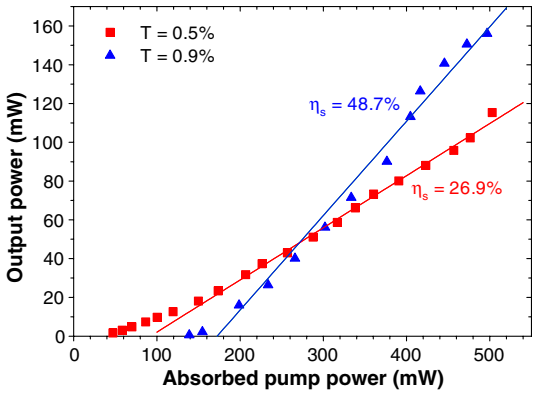

Fig. 4. (Color online) Output power versus absorbed pump power for two output coupler transmissions.

4. CONCLUSION

In conclusion, we have demonstrated a compact and efficient InGaN laser diode-pumped Pr:YLF laser at 698 nm using a simple plano-concave cavity. A maximum output power of 156 mW was obtained in a single transverse mode with a slope efficiency as high as 48.7%. Power scaling is still expected if higher pump power is injected. The laser performance can be also improved by further optimization of the resonator output coupling and by work on Pr:YLF laser crystals with antireflection coatings and optimized doping concentrations. The $^3P_0 \rightarrow {}^3F_3$ transition of Pr:YLF has potential application for the Sr-based optical lattice clock. Furthermore, we believe that the second-harmonic generation at 349 nm could be achieved, which is expected to produce higher conversion efficiency compared with other less efficient techniques such as third-harmonic generation in a Nd:YLF laser crystal.

ACKNOWLEDGMENTS

This work is financially supported by the National Natural Science Foundation of China (No. 61275050) and the Xiamen Scientific & Technologic Project (No. 3502Z20113004).

REFERENCES

1. F. Cornacchia, A. Richter, E. Heumann, G. Huber, D. Parisi, and M. Tonelli, "Visible laser emission of solid state pumped $LiLuF_4$:Pr^{3+}," Opt. Express **15**, 992–1002 (2007).
2. B. Xu, P. Camy, J. L. Doualan, A. Braud, Z. Cai, F. Balembois, and R. Moncorgé, "Frequency doubling and sum-frequency mixing operation at 469.2, 471, and 473 nm in Nd:YAG," J. Opt. Soc. Am. B **29**, 346–350 (2012).
3. B. Xu, P. Camy, J. L. Doualan, Z. Cai, and R. Moncorgé, "Visible laser operation of Pr^{3+}-doped fluoride crystals pumped by a 469 nm blue laser," Opt. Express **19**, 1191–1197 (2011).
4. A. Richter, E. Heumann, E. Osiac, G. Huber, W. Seelert, and A. Diening, "Diode pumping of a continuous-wave Pr^{3+}-doped $LiYF_4$ laser," Opt. Lett. **29**, 2638–2640 (2004).
5. K. Hashimoto and F. Kannari, "High-power GaN diode-pumped continuous wave Pr^{3+}-doped $LiYF_4$ laser," Opt. Lett. **32**, 2493–2495 (2007).
6. F. Cornacchia, A. Di Lieto, M. Tonelli, A. Richter, E. Heumann, and G. Huber, "Efficient visible laser emission of GaN laser diode pumped Pr-doped fluoride scheelite crystals," Opt. Express **16**, 15932–15941 (2008).
7. D. Pabœuf, O. Mhibik, F. Bretenaker, P. Goldner, D. Parisi, and M. Tonelli, "Diode-pumped Pr:BaY_2F_8 continuous-wave orange laser," Opt. Lett. **36**, 280–282 (2011).
8. P. Camy, J. L. Doualan, R. Moncorgé, J. Bengoechea, and U. Weichmann, "Diode-pumped Pr^{3+}:KY_3F_{10} red laser," Opt. Lett. **32**, 1462–1464 (2007).
9. M. Fibrich, H. Jelinková, J. Šulc, K. Nejezchleb, and V. Škoda, "Visible cw laser emission GaN-diode pumped Pr:$YAlO_3$ crystal," Appl. Phys. B**97**, 363–367 (2009).
10. T. Calmano, J. Siebenmorgen, F. Reichert, M. Fechner, A.-G. Paschke, N.-O. Hansen, K. Petermann, and G. Huber, "Crystalline Pr:$SrAl_{12}O_{19}$ waveguide laser in the visible spectral region," Opt. Lett. **36**, 4620–4622 (2011).
11. H. Okamoto, K. Kasuga, I. Hara, and Y. Kubota, "Visible–NIR tunable Pr^{3+}-doped fiber laser pumped by a GaN laser diode," Opt. Express **17**, 20227–20232 (2009).
12. J. Nakanishi, Y. Horiuchi, T. Yamada, O. Ishii, M. Yamazaki, M. Yoshida, and Y. Fujimoto, "High-power direct green laser oscillation of 598 mW in Pr^{3+}-doped waterproof fluoroaluminate glass fiber excited by two-polarization-combined GaN laser diodes," Opt. Lett. **36**, 1836–1838 (2011).
13. T. Gün, P. Metz, and G. Huber, "Power scaling of laser diode pumped Pr^{3+}:$LiYF_4$ cw lasers: efficient laser operation at 522.6 nm, 545.9 nm, 607.2 nm, and 639.5 nm," Opt. Lett. **36**, 1002–1004 (2011).
14. M. G. Tarallo, N. Poli, M. Schioppo, D. Sutyrin, and G. M. Tino, "A high-stability semiconductor laser system for a ^{88}Sr-based optical lattice clock," Appl. Phys. B **103**, 17–25 (2011).
15. T. Sandrock, T. Danger, E. Heumann, G. Huber, and B. H. T. Chai, "Efficient continuous wave-laser emission of Pr^{3+}-doped fluorides at room temperature," Appl. Phys. B **58**, 149–151 (1994).
16. J. M. Sutherland, P. M. W. French, J. R. Taylor, and B. H. T. Chai, "Visible continuous-wave laser transitions in Pr^{3+}:YLF and femtosecond pulse generation," Opt. Lett. **21**, 797–799 (1996).